THE ASTROPHYSICAL JOURNAL, **238**:1066–1080, 1980 June 15

EXACT AND APPROXIMATE SOLUTIONS FOR THE ONE-DIMENSIONAL TRANSFER OF POLARIZED RADIATION, AND APPLICATIONS TO X-RAY PULSARS

P. MÉSZÁROS,[1] W. NAGEL,[2] AND J. VENTURA[2]
Max-Planck-Institut für Physik und Astrophysik
Received 1979 October 23; accepted 1979 December 13

ABSTRACT

Theoretical studies of the radiation from hot, strongly magnetized plasmas, as encountered in pulsars, require a knowledge of solutions to the transfer equations for polarized radiation. We present here an analytic solution of the radiative transfer equations for one-dimensional propagation across a homogeneous slab of finite depth, as well as for a semi-infinite atmosphere. Absorption, scattering, and mode-exchange between the two polarizations are included, the role of the last being crucial. A physical discussion of the solutions for certain limiting cases and an interpretation in terms of probabilistic (quantum escape approach) arguments corroborate these solutions, and provide a better intuitive feel for the behavior of the radiated spectra. Whereas our analytic solutions are valid for any birefringent medium (not necessarily magnetic), our numerical examples and the qualitative discussion presented refer to the particular problem of the radiation from X-ray pulsars. Large-scale qualitative and quantitative changes from the nonmagnetic spectra are found, which affect both the continuum and the spectral lines.

Subject headings: polarization — pulsars — radiative transfer — X-rays: general

I. INTRODUCTION

Spectral characteristics of individual sources have long been used in X-ray astronomy to isolate candidates for X-ray pulsars in binary systems. The discovery of the binary nature of SMC X-1 (Schreier *et al.* 1972) is a good example of this. Indeed, if the galactic X-ray sources are plotted on a "two-color" plot, the pulsars are easily seen to form a class by themselves having a harder spectrum than the other galactic sources (Ostriker 1977). Nevertheless, until now there was no systematic theoretical work appropriate for analyzing the observed spectra of X-ray pulsars, currently thought to be accreting magnetic neutron stars. Early theoretical work on nonmagnetic sources (Felten and Rees 1972) has shown that the expected spectra can differ widely from the blackbody law in the X-ray frequency range. This has turned out to be the case with most of the observed spectra (Jones 1977; Markert *et al.* 1979), which in addition show a considerable variety of detail hitherto unexplored.

The presence of the pulsar magnetic field changes not only the geometry of accretion, but also the physics of the radiation diffusion in the lower accretion funnel. One has to deal with two normal modes of propagation with widely different anisotropic and frequency-dependent opacities (Canuto, Lodenquai, and Ruderman 1971; Lodenquai *et al.* 1974; Gnedin, Pavlov, and Shibanov 1978). Under such circumstances the spectra from magnetized objects are expected to differ widely from those of nonmagnetic media. This expectation is indeed strengthened after the exciting recent discovery of cyclotron line features in the hard X-ray spectra of the pulsars Her X-1 and 4U 0115+63 (Trümper *et al.* 1978; Voges *et al.* 1979; Wheaton *et al.* 1979).

One of the necessary ingredients for the proper modeling of these objects is an accurate knowledge of the transfer of radiation through birefringent magnetic media. This problem arises in several other areas of astrophysics as well as in materials physics. General transfer equations have been given by, for example, Chandrasekhar (1960), Sobolev (1963), and Gnedin and Pavlov (1974), while solutions of these have been obtained for specialized problems mostly in radio astronomy (e.g., Ginzburg, Sazonov and Syrovatsky 1968; Zheleznyakov 1970; Pacholczyk 1977) and in connection with magnetic white dwarfs (Lamb and Sutherland 1974; Masters *et al.* 1977).

We have recently undertaken a comprehensive study of the spectral and polarization properties expected in the radiation from hot birefringent media in the limit of strong Faraday depolarization of the two normal modes of propagation (Gnedin and Pavlov 1974). Using for our analysis recent results for the Thomson and free-free opacities in magnetized plasmas, we find that *qualitative and quantitative* deviations from the nonmagnetic spectra follow because mode-exchange scattering is efficient as compared to bremsstrahlung absorption. Partial results previously reported by us have focused on the physics of cyclotron line formation (Nagel 1980) and on the effect of vacuum polarization (Ventura, Nagel, and Mészáros 1979, hereafter Paper I).

[1] Institut für Astrophysik.

[2] Institut für Extraterrestrische Physik.

Here we discuss the radiative transfer in a one-dimensional birefringent medium, giving exact and approximate solutions for the diffuse reflection and transmission coefficients in the case of coherent photon scattering. These results are valid for *any* homogeneous, birefringent medium (not necessarily gaseous or magnetized), as long as Comptonization can be neglected, and the limit of large Faraday depolarization applies. We then apply our results specifically to the transfer problem in an X-ray pulsar, which we idealize to that of a homogeneous radiating slab illuminated on one side by a blackbody flux. Our results hold the promise of distinguishing between magnetic and nonmagnetic X-ray sources from the study of their X-ray and UV spectra alone.

II. PHOTON OPACITIES IN A MAGNETIZED PLASMA

The presence of a strong magnetic field severely affects the photon opacities, which become extremely dependent on the photon's polarization, frequency, and direction of propagation (Lodenquai *et al.* 1974; Gnedin and Sunyaev 1973). In the UV and X-ray range of frequencies, a plasma of moderate density and temperature ($n_e \lesssim 10^{23}$ cm^{-3}, $T \lesssim 10$ keV) is only weakly dispersive, with practically transverse normal modes of propagation obeying the dispersion relation of a cold electron plasma. For very strong magnetic fields, vacuum polarization begins to modify significantly the normal modes at frequencies $\omega \gtrsim \omega_v = 1.5$ keV $(n_e/10^{20}\ \text{cm}^{-3})^{1/2}\,(B/10^{12}\ \text{gauss})^{-1}$, where B is the external field, and n_e the electron number density (Mészáros and Ventura 1978, 1979; Gnedin, Pavlov, and Shibanov 1978). In either case there are two normal modes (called ordinary and extraordinary in the cold plasma limit), which are mutually orthogonal to a good approximation.

The scattering ($\sigma_{1,2}$) and absorption coefficients ($\kappa_{1,2}$) for the two modes are widely different, as can be seen from Figure 1, which depicts angular averages of the cross sections as a function of frequency. Only the extraordinary mode (mode 1) exhibits a resonance at the cyclotron frequency, assumed here to be $\omega_H = 50$ keV, if vacuum polarization can be neglected. At frequencies much below the cyclotron frequency, $\omega \ll \omega_H$, the cross sections for photons of mode 1 are distinctly suppressed compared with mode 2, $\kappa_1/\kappa_2 \approx \sigma_1/\sigma_2 \approx (\omega/\omega_H)^2$. Details of this calculation have been given in previous papers (Ventura 1979; and Paper I, where some effects of vacuum polarization were also discussed).

For either mode the absorption coefficient exceeds the scattering coefficient at low frequencies, i.e., $\kappa_i \gg \sigma_i$ ($i = 1, 2$), while this inequality is reversed at high frequencies. In the case of a pure hydrogen plasma with temperature $T \sim 10$ keV this reversal occurs at $\omega_b \sim 0.04$ keV $(n_e/10^{22}\ \text{cm}^{-3})^{1/2}$ (cf. Fig. 1). Following equations (1)–(3) in Paper I we can derive an approximate expression for the ratio κ/σ, valid over the entire range of frequencies and angles of propagation:

$$\frac{\kappa_1}{\sigma_1} \sim \frac{\kappa_2}{\sigma_2} \sim \frac{3\pi}{2}\, g\, \frac{Ze^2}{\hbar v_T}\, n_e \frac{c^3}{\omega^3}\,(1 - e^{-\hbar\omega/kT})\,. \tag{1}$$

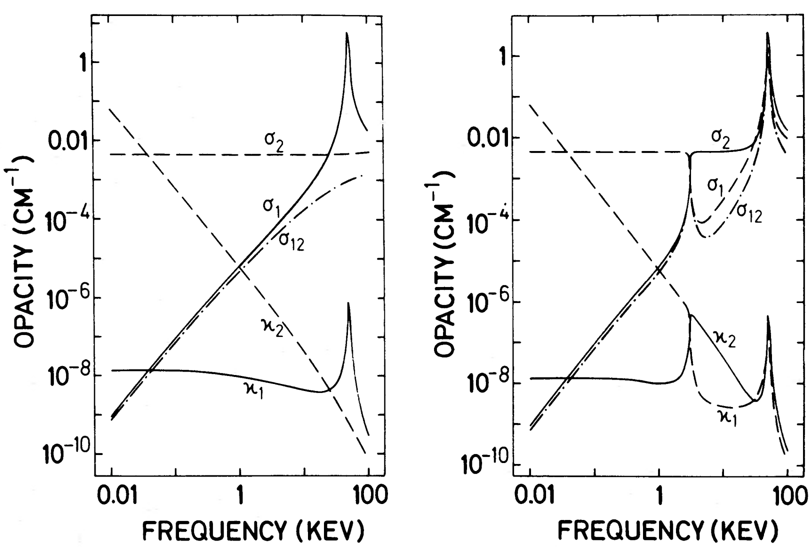

FIG. 1.—Scattering (σ) and absorption (κ) coefficients for extraordinary (1) and ordinary (2) photons in a strongly magnetized plasma of (electron) density 10^{22} cm^{-3} and temperature 10 keV. The polarization exchange coefficients $\sigma_{12} = \sigma_{21}$ are also indicated. With these parameters the crossover from the absorption-dominated ($\kappa \gg \sigma$) to the scattering-dominated ($\kappa \ll \sigma$) regime occurs at the frequency $\hbar\omega_b \approx 0.04$ keV. The "strong-coupling regime" (see § III) extends from $\hbar\omega_b' \approx 1$ keV to the highest frequencies. The magnetic field strength is $B = 4.4 \times 10^{12}$ gauss. Fig. 1(*a*) gives the cross sections as calculated with the usual cold plasma modes; Fig. 1(*b*) includes the effect of vacuum polarization on the normal modes.

Here Z is the ion atomic number, g is a Gaunt factor, and $v_T = (\pi kT/2m)^{1/2}$ is the electron thermal velocity. It is assumed that the electron velocities along the magnetic field obey a Maxwellian distribution, characterized by a temperature $T = T_{\|}$, ($kT \ll \hbar\omega_H$). However, the transverse distribution, i.e. the occupation of the Landau levels, need not be given by the same temperature; it may not even be an equilibrium distribution. Under the conditions discussed here, the rate of Coulomb excitation or de-excitation in the plasma is negligible compared to the radiative de-excitation rate of the Landau levels. Thus the occupation of the Landau levels will not be controlled by collisions (and hence by the longitudinal temperature T), but rather by the density of photons having energies near $\hbar\omega_H$.

Equation (1) establishes that, apart from details in the (slowly varying) Gaunt factor, the ratio κ/σ has the same frequency dependence in the magnetic and nonmagnetic cases. The probability,

$$\epsilon_i = \frac{\kappa_i}{\kappa_i + \sigma_i} \tag{2}$$

that a photon in mode i will be thermalized (absorbed) during a single interaction event is thus roughly independent of polarization, and for our qualitative estimates we shall assume $\epsilon_1 = \epsilon_2 = \epsilon$. Since the purpose of the present computation is mainly to elucidate the physics and ground rules for the transfer of polarized radiation, we prefer to keep the cross sections as simple as possible, assuming $g = 1$ for the Gaunt factors and neglecting the effect of vacuum polarization. Inclusion of these effects is straightforward and was fully taken into account in Paper I.

III. HEURISTIC TREATMENT OF THE RADIATIVE TRANSFER PROBLEM

The absorption probability ϵ is a parameter of paramount importance in any radiative transfer problem. If $\epsilon \approx 1$, a semi-infinite homogeneous atmosphere will radiate like a blackbody,

$$I \sim B\,, \tag{3a}$$

whereas for $\epsilon \ll 1$ the emergent intensity, in the case of a one-dimensional medium, is

$$I \sim 2\epsilon^{1/2} B \tag{3b}$$

(e.g., Sobolev 1963). The term B denotes here the Planck specific intensity. Felten and Rees (1972) have given a very appealing intuitive argument for the appearance of the factor $\epsilon^{1/2}$ in formula (3b). Only photons created in a surface layer of depth $x_{\rm th}$, which is called the thermalization length, have a significant chance to escape. The flux of emergent photons can be estimated by multiplying this length $x_{\rm th}$ by the production rate of photons per unit depth of the medium:

$$I \sim \kappa B x_{\rm th}\,. \tag{4}$$

If $\epsilon \approx 1$, the thermalization length is simply κ^{-1}, so that one recovers $I \approx B$. In the case $\epsilon \ll 1$, i.e., $\kappa \ll \sigma$, the photons are scattered many times before they escape. The number of steps is of the order $N \approx \epsilon^{-1} \sim \sigma/\kappa$, and the mean distance traveled between two scattering events is σ^{-1}. Hence the total distance over which a photon can diffuse is given by

$$x_{\rm th} \approx N^{1/2}\sigma^{-1} \sim (\sigma\kappa)^{-1/2}$$

and the emergent flux is estimated to be

$$I \sim \kappa B(\sigma\kappa)^{-1/2} = (\kappa/\sigma)^{1/2} B\,.$$

The extra factor 2 in formula (3b) is due to the photons which are initially produced in the inward direction. Since in the case $\epsilon \ll 1$ the medium is strongly reflecting, photons traveling inward have nearly the same chance of escaping as those traveling outward. On the other hand, for $\epsilon \approx 1$, the reflectivity is low, and thus the factor 2 is absent in formula (3a).

How should this argument be modified if two types of photons, with drastically different opacities, can propagate in the medium? A medium subject to the opacities σ_1 and σ_2 and to the mode-exchange probabilities σ_{21}/σ_1 and σ_{12}/σ_2 is a natural polarizer. At frequencies well below the cyclotron resonance, where $\sigma_2 \gg \sigma_1$, a magnetized slab of finite dimension could be transparent to mode 1 and optically thick to mode 2. Of an unpolarized incident beam, mode 1 would readily go through the slab, whereas mode 2 photons would scatter σ_2/σ_{12} times (in the average) re-emerging on both sides, mostly in mode 1, after mode-exchange scattering.

The importance of mode exchange on the radiative transfer is thus immediately clear. Depending on the effectiveness of mode exchange, the transport of radiation occurs in a qualitatively different manner in the following three cases.

a) *Weak Coupling:* $\sigma_{12} \ll \kappa_1, \kappa_2$

Photons in this case are likely to be absorbed in the same polarization state in which they were produced. Hence the two types of photons diffuse independently, and we can immediately apply the above argument to each mode. We easily see that two separate thermalization lengths are obtained ($i = 1, 2$),

$$x_i = (\kappa_i \sigma_i)^{-1/2} = \epsilon^{1/2} \kappa_i^{-1} \quad (\epsilon \ll 1), \qquad x_i \approx \kappa_i^{-1} \quad (\epsilon \approx 1), \tag{5}$$

and the radiated intensities are

$$I_i \approx 2 x_i \kappa_i B \approx 2\epsilon^{1/2} B \quad (\epsilon \ll 1), \qquad I_i \approx x_i \kappa_i B \approx B \quad (\epsilon \approx 1). \tag{6}$$

As already discussed in connection with equations (1) and (2), ϵ is a smooth function of the frequency differing only slightly from the nonmagnetic case.

These considerations establish that if the coupling of the two modes is neglected in the scattering-dominated range of frequencies, use of the magnetic field opacities σ_i and κ_i would still lead at *infinite optical depth* to spectra very similar to those of the nonmagnetic case. There would thus be no cyclotron spectral feature, since the increased production rate in equation (6) would be exactly offset by the decreased depth of escape. We shall see that these results are drastically changed when the coupling of the normal modes is included.

b) *Case of Intermediate Coupling:* $\kappa_1 \ll \sigma_{12} \ll \kappa_2$

In Figure 1, this case is encountered at an intermediate range of frequencies of 0.04–1 keV. At these frequencies, type 2 photons are the main source of radiation. They can escape after repeated scattering as 2-photons from within a skin of dimension $x_2 = (\kappa_2 \alpha_2)^{-1/2}$, where $\alpha_i \equiv \kappa_i + \sigma_i$ is the total opacity. These photons also escape as 1-photons from within a deeper range, $x_{21} = (\alpha_1 \sigma_{12})^{-1/2} \approx \alpha_1^{-1}$. The radiated intensity is

$$I_2 \approx B\kappa_2 x_2 \approx \epsilon^{1/2} B \tag{7}$$

for the first case, and for the second case

$$I_1 \approx B\kappa_2 P_{12} x_{21},$$

where $P_{12} = (\alpha_2/\kappa_2)(\sigma_{12}/\alpha_2)$ is the probability for a $2 \rightarrow 1$ conversion of photons having scattered a mean number $\alpha_2/\kappa_2 \approx \epsilon^{-1}$ of times. The result is

$$I_1 = B(\sigma_{12}/\alpha_1)^{1/2} \sim B. \tag{8}$$

Mode 2 would thus have a "spectral break" at $\omega_b \sim 0.04$ keV, and exhibit a spectrum very similar to the Felten and Rees spectrum, whereas I_1 would continue along the blackbody line, well beyond ω_b, up to the frequency $\omega_{b'} \approx (\omega_b \omega_H)^{1/2}$.

c) *Strong Coupling:* $\kappa_1, \kappa_2 \ll \sigma_{12}$

Prior to escape a photon generally experiences multiple scatterings and conversions, the total number of which cannot exceed ϵ^{-1} (else it is absorbed). If the two modes have very different opacities, say $\alpha_2 \gg \alpha_1$, absorption would occur principally in mode 2, while mode 1 is the principal mode of photon diffusion and escape. This happens because mode-2 scattering is relatively localized within a length of dimension

$$x_{12} = (\sigma_{12}\alpha_2)^{-1/2} \sim \alpha_1^{-1}(\alpha_1/\alpha_2)^{1/2} \ll \alpha_1^{-1},$$

corresponding to an average of α_2/σ_{12} scatterings (cf. Fig. 2). The thermalization length of a photon is then easily estimated to be

$$x_{\text{th}} = x_1 \approx x_2 = (\kappa_2 \alpha_1)^{-1/2}, \tag{9}$$

while the radiated intensities are

$$I_1 + I_2 \approx B(\kappa_1 + \kappa_2) x_{\text{th}} \approx (\epsilon \alpha_2/\alpha_1)^{1/2} B, \qquad I_2/I_1 \approx (\sigma_{12}/\alpha_2)^{1/2}. \tag{10}$$

To verify the second of these equations, one has to consider the main contributions to I_2 in some detail. One contribution comes from photons created in mode 2 within the outer skin depth x_{12}, while a second and dominant one comes from mode-1 photons, which have a finite probability $\sim \sigma_{12} x_{12}$ for converting into mode 2, as they traverse the outer skin depth x_{12}.

We thus see that highly polarized radiation, dominated by mode-1 photons, is expected from an optically thick slab. The lower intensity is $I_2 \approx \epsilon^{1/2} B_\omega$, following close to the usual limiting luminosity for unmagnetized media. The intensity I_1, however, exceeds this limit by a factor $\sim(\alpha_2/\alpha_1)^{1/2} \gg 1$. Higher overall intensities should thus

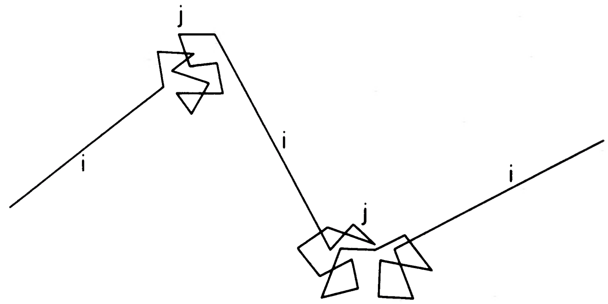

FIG. 2.—In the "strong-coupling regime" a typical photon history involves several scatterings from a mode (i) with a long mean free path to the other mode (j) having a short mean free path.

characterize the coherent spectra of magnetized matter. Spectral line features resembling emission or absorption lines are also predicted whenever the opacity ratio α_2/α_1 goes through sharp variations with changing frequency (see Nagel 1980; Paper I).

These qualitative results are verified by the exact solutions for the transfer in a birefringent one-dimensional medium depicted in Figure 3, the results for which (cf. § VI) are shown in Figure 4. Since the radiative transfer problem in a plane-parallel atmosphere can be approximately reduced to that of the one-dimensional case (Sobolev 1963), such exact solutions can be of great value. We devote the following sections to this problem.

IV. THE TRANSFER EQUATION

We use a form of the transfer equation derived by Gnedin and Pavlov (1974), which reduces the problem to the determination of radiation intensities in the two normal modes of the medium. This equation is specialized to a one-dimensional medium, which should serve as a model for the radiation transport in a slab of finite thickness z_0. Hence we ignore the angular distribution of photons and introduce simply the upward and downward flux of photons in each mode. Thus, e.g., I_2^- is to represent the flux of photons of type 2 in the direction of increasing depth z (see Fig. 3). Defining the opacities $\alpha_i = \sigma_i + \kappa_i$ as the sum of scattering (σ_i) and absorption coefficients (κ_i) for photons in mode i, we obtain the following transfer equations:

$$
\begin{aligned}
-\frac{dI_1^+}{dz} &= -\alpha_1 I_1^+ + \tfrac{1}{2}\sigma_{11}(I_1^+ + I_1^-) + \tfrac{1}{2}\sigma_{12}(I_2^+ + I_2^-) + \kappa_1 B\,,\\
\frac{dI_1^-}{dz} &= -\alpha_1 I_1^- + \tfrac{1}{2}\sigma_{11}(I_1^+ + I_1^-) + \tfrac{1}{2}\sigma_{12}(I_2^+ + I_2^-) + \kappa_1 B\,,\\
-\frac{dI_2^+}{dz} &= -\alpha_2 I_2^+ + \tfrac{1}{2}(I_1^+ + I_1^-) + \tfrac{1}{2}\sigma_{22}(I_2^+ + I_2^-) + \kappa_2 B\,,\\
\frac{dI_2^-}{dz} &= -\alpha_2 I_2^- + \tfrac{1}{2}\sigma_{21}(I_1^+ + I_1^-) + \tfrac{1}{2}\sigma_{22}(I_2^+ + I_2^-) + \kappa_2 B\,.
\end{aligned}
\qquad (11)
$$

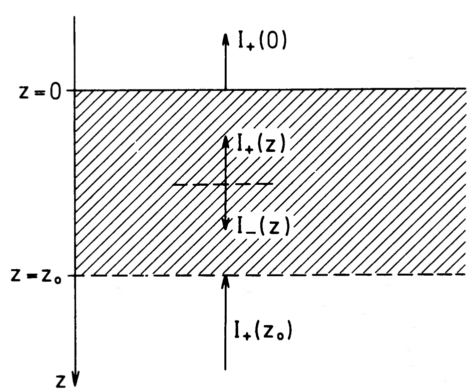

FIG. 3.—The one-dimensional transfer model used for calculating all the spectra shown in this paper. The graphs display $I_+(0)$, the flux escaping through the upper boundary (toward the observer). The flux of photons entering the slab from below (background illumination) is designated by $I_+(z_0)$.

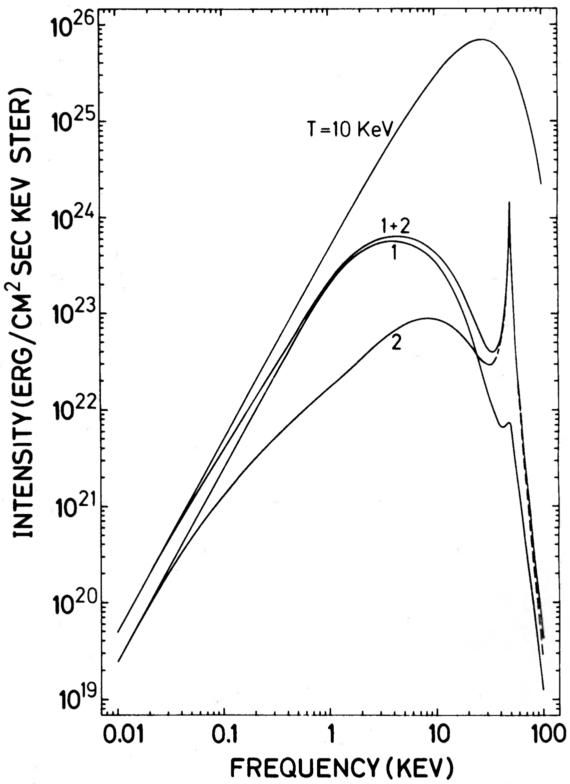

FIG. 4.—Radiation from a semi-infinite medium of density $n_e = 10^{22}$ cm^{-3}, in which two types of photons can propagate, with the cross sections depicted in Fig. 1(*a*). The top curve represents blackbody emission at the slab temperature of $T = 10$ keV.

The coefficients σ_{ij} are the coefficients for scattering a photon from mode j into mode i, and have the property $\sigma_i = \sigma_{1i} + \sigma_{2i}$. We assume the scattering of photons to be equally probable in the forward and backward directions, hence the factors $\frac{1}{2}$ in equations (11). It is convenient to introduce the density $J_i = I_i^+ + I_i^-$ and flux $F_i = I_i^+ - I_i^-$ of photons of type i. Adding and subtracting the first two of equations (11) we get

$$\frac{dJ_1}{dz} = \alpha_1 F_1 , \tag{12a}$$

$$\frac{dF_1}{dz} = \alpha_1 J_1 - \sigma_{11} J_1 - \sigma_{12} J_2 - 2\kappa_1 B . \tag{12b}$$

Of course, there are two similar equations for J_2 and F_2. We can use equation (12a) to eliminate the flux F_1, arriving at a diffusion equation for J_1; with $\alpha_1{}^{-1}$ playing the role of the diffusion coefficient (see Nagel 1980):

$$\alpha_1{}^{-1} \frac{d^2 J_1}{dz^2} = \alpha_1 J_1 - \sigma_{11} J_1 - \sigma_{12} J_2 - 2\kappa_1 B . \tag{13}$$

Defining the matrices

$$\boldsymbol{\alpha} = \begin{pmatrix} \alpha_1 & 0 \\ 0 & \alpha_2 \end{pmatrix}, \quad \boldsymbol{\sigma} = \begin{pmatrix} \sigma_{11} & \sigma_{12} \\ \sigma_{21} & \sigma_{22} \end{pmatrix}, \quad \boldsymbol{\kappa} = \begin{pmatrix} \kappa_1 & 0 \\ 0 & \kappa_2 \end{pmatrix}, \tag{14}$$

and the vectors $\boldsymbol{J} = (J_1, J_2)^T$, $\boldsymbol{J}^* = (2B, 2B)^T$ (LTE photon-density), we can combine equation (13) with its corresponding form for J_2 into the matrix equation

$$\boldsymbol{\alpha}^{-1} \frac{d^2}{dz^2} \boldsymbol{J} = (\boldsymbol{\alpha} - \boldsymbol{\sigma})\boldsymbol{J} - \boldsymbol{\kappa}\boldsymbol{J}^* , \tag{15}$$

describing the transfer of two polarizations.

If the coefficients $\boldsymbol{\alpha}$, $\boldsymbol{\sigma}$, and $\boldsymbol{\kappa}$ do not depend on the depth z, the transfer equation (15) is easily solved with the ansatz

$$\boldsymbol{J} = \boldsymbol{u}e^{-\lambda z} . \tag{16}$$

This leads to the eigenvalue problem

$$\boldsymbol{\alpha}(\boldsymbol{\alpha} - \boldsymbol{\sigma})\boldsymbol{u} = \lambda^2 \boldsymbol{u} , \tag{17}$$

from which we can calculate two eigenvectors, $\boldsymbol{u}$ and $\boldsymbol{v}$, belonging to the two eigenvalues λ^2 and μ^2:

$$\left.\begin{matrix}\lambda^2\\ \mu^2\end{matrix}\right\} = \frac{\alpha_1(\alpha_1 - \sigma_{11}) + \alpha_2(\alpha_2 - \sigma_{22})}{2} \pm \left\{\left[\frac{\alpha_1(\alpha_1 - \sigma_{11}) - \alpha_2(\alpha_2 - \sigma_{22})}{2}\right]^2 + \sigma_{12}\sigma_{21}\alpha_1\alpha_2\right\}^{1/2} . \tag{18}$$

The general solution can be written as a superposition of the form

$$\boldsymbol{J} = \boldsymbol{J}^* - (c_1 e^{-\lambda z} + c_2 e^{\lambda z})\boldsymbol{u} - (d_1 e^{-\mu z} + d_2 e^{\mu z})\boldsymbol{v} . \tag{19}$$

The boundary conditions

$$I_{1,2}^-(z = 0) = 0 , \qquad I_{1,2}^+(z = z_0) = I_{\mathrm{inc}_{1,2}} , \tag{20}$$

can be expressed in terms of J and the derivatives dJ/dz as follows:

$$I_i^{\pm} = \frac{1}{2}(J_i \pm F_i) = \frac{1}{2}\left(J_i \pm \alpha_i^{-1}\frac{dJ_i}{dz}\right) . \tag{21}$$

Substituting into this the general solution (19) leads to a system of four equations for the unknown coefficients $c_{1,2}$ and $d_{1,2}$ which can be solved by standard methods.

Though simple in principle (and numerically), it is tedious to solve these equations for the four unknowns and to substitute the coefficients back into the general solution to find analytic expressions for the emergent intensities I_1^+ $(z = 0)$ and I_2^+ $(z = 0)$. We give the details of this exact solution in the Appendix. Here, in order to get some insight and avoid extended formulae, we discuss next a semi-infinite atmosphere ($z_0 \to \infty$), in which case $c_2 = d_2 = 0$ and we are left with a two-by-two system.

V. THE CASE OF A SEMI-INFINITE ATMOSPHERE

We shall not try to attack these two equations for the coefficients c_1 and d_1 directly. Instead, we derive a formal solution first, using the concept of the photon escape probability introduced by Sobolev (1963). Thus we define a matrix

$$\mathbf{p}(z) = \begin{pmatrix} p_{11}(z) & p_{12}(z) \\ p_{21}(z) & p_{22}(z) \end{pmatrix} , \tag{22}$$

$p_{12}(z)$, for example, giving the probability that a photon released at depth z in mode 2 will eventually escape from the atmosphere as a type-1 photon. The probability of direct escape (without undergoing any scattering) is given by the matrix

$$\frac{1}{2}e^{-\boldsymbol{\alpha} z} = \frac{1}{2}\begin{pmatrix} \exp(-\alpha_1 z) & 0 \\ 0 & \exp(-\alpha_2 z) \end{pmatrix} , \tag{23}$$

the factor $\frac{1}{2}$ arising from the assumption that the photons are released with equal probabilities in the upward or downward direction. Since a photon either escapes directly or after at least one scattering process, it is obvious that $\mathbf{p}(z)$ must satisfy the following integral equation:

$$\mathbf{p}(z) = \tfrac{1}{2}e^{-\boldsymbol{\alpha} z} + \int_0^\infty dz' \mathbf{p}(z')\tfrac{1}{2}\boldsymbol{\sigma} e^{-\boldsymbol{\alpha}|z' - z|} . \tag{24}$$

Differentiating twice we find that this is equivalent to the differential equation

$$\frac{d^2}{dz^2}\mathbf{p} = \mathbf{p}(\boldsymbol{\alpha} - \boldsymbol{\sigma})\boldsymbol{\alpha} , \tag{25}$$

and the boundary conditions

$$\frac{d}{dz}\mathbf{p}(z=0) = \mathbf{p}(0)\boldsymbol{\alpha} - \boldsymbol{\alpha}\,, \qquad \mathbf{p}(z\to\infty)\to 0\,. \tag{26}$$

It is easy to see that the differential equation (25) is satisfied by

$$\mathbf{p} = \mathbf{p}_0 e^{-\boldsymbol{\Lambda} z}\,, \tag{27}$$

where $\boldsymbol{\Lambda} = [(\boldsymbol{\alpha} - \boldsymbol{\sigma})\boldsymbol{\alpha}]^{1/2}$ is the positive root of $(\boldsymbol{\alpha} - \boldsymbol{\sigma})\boldsymbol{\alpha}$, i.e., it has positive eigenvalues. It turns out that these eigenvalues are just λ and μ defined in equation (18) above. Of course this was to be expected since equation (27) is just a different description of the same problem. The matrix $\mathbf{p}_0$, giving the escape probability at the surface, is obtained from the boundary condition (26):

$$-\mathbf{p}_0\boldsymbol{\Lambda} = \mathbf{p}_0\boldsymbol{\alpha} - \boldsymbol{\alpha}\,, \tag{28}$$

i.e.,

$$\mathbf{p}_0 = \boldsymbol{\alpha}(\boldsymbol{\alpha} + \boldsymbol{\Lambda})^{-1}\,. \tag{29}$$

This quantity is simply related to the reflectivity $\mathbf{r}_0$ of the atmosphere. Since a photon is created either upward or downward, its escape probability is

$$\mathbf{p}_0 = \tfrac{1}{2} + \tfrac{1}{2}\mathbf{r}_0 \tag{30}$$

and thus

$$\mathbf{r}_0 = (\boldsymbol{\alpha} - \boldsymbol{\Lambda})(\boldsymbol{\alpha} + \boldsymbol{\Lambda})^{-1}\,. \tag{31}$$

Photons are produced thermally at a rate $2\kappa_1 B$ and $2\kappa_2 B$. Hence the flux of photons escaping from the atmosphere is given by

$$\begin{pmatrix} I_1^{+}(0) \\ I_2^{+}(0) \end{pmatrix} = \int_0^\infty dz \begin{pmatrix} p_{11}(z) & p_{12}(z) \\ p_{21}(z) & p_{22}(z) \end{pmatrix} \begin{pmatrix} 2\kappa_1 B \\ 2\kappa_2 B \end{pmatrix}. \tag{32}$$

Denoting by $F_i = I_i^{+}(0)/B$ the ratio of the emergent intensity to the blackbody intensity (per mode), and defining the vector $\boldsymbol{\kappa} = (\kappa_1, \kappa_2)$, we can write

$$\boldsymbol{F} = 2\mathbf{C}\boldsymbol{\kappa}\,, \tag{33}$$

where the matrix $\mathbf{C}$ is given by

$$\mathbf{C} = \int_0^\infty dz\mathbf{p}(z) = \int_0^\infty dz\mathbf{p}_0 e^{-\boldsymbol{\Lambda} z} = \mathbf{p}_0\boldsymbol{\Lambda}^{-1}\,. \tag{34}$$

Using the expression (29) for $\mathbf{p}_0$ one finds

$$\mathbf{C} = \boldsymbol{\alpha}(\boldsymbol{\Lambda}\boldsymbol{\alpha} + \boldsymbol{\Lambda}^2)^{-1} = (\boldsymbol{\Lambda} + \boldsymbol{\alpha} - \boldsymbol{\sigma})^{-1}\,. \tag{35}$$

Equation (33) provides the justification of the procedure used in Paper I for estimating the emissivity of a strongly scattering medium in which two types of photons can propagate. The matrix elements C_{ij} give the mean depth from which a photon that was born in state j can escape, suitably weighted with its probability to escape as a type-i photon. We will now derive explicit formulae from the formal expression (35). Since there are only two normal modes, we have $\alpha_1 - \sigma_{11} = \sigma_{21} + \kappa_1$, and $\alpha_2 - \sigma_{22} = \sigma_{12} + \kappa_2$; thus

$$(\boldsymbol{\alpha} - \boldsymbol{\sigma})\boldsymbol{\alpha} = \begin{pmatrix} (\sigma_{21} + \kappa_1)\alpha_1 & -\sigma_{12}\alpha_2 \\ -\sigma_{21}\alpha_1 & (\sigma_{12} + \kappa_2)\alpha_2 \end{pmatrix}. \tag{36}$$

Quite generally, the square root of a positive definite two-by-two matrix

$$\mathbf{A} = \begin{pmatrix} a_{11} & a_{12} \\ a_{21} & a_{22} \end{pmatrix} \tag{37}$$

is given by

$$(\mathbf{A})^{1/2} = N^{-1/2}\begin{pmatrix} a_{11} + (d)^{1/2} & a_{12} \\ a_{21} & a_{22} + (d)^{1/2} \end{pmatrix}, \tag{38}$$

with $d = a_{11}a_{22} - a_{12}a_{21}$, and $N = a_{11} + a_{22} + 2(d)^{1/2}$.

We apply this formula to matrix (36) and discuss the resulting expression in the three different parameter regimes introduced in § III.

a) Weak-Coupling Case: $\kappa_1, \kappa_2 \gg \sigma_{12}$

In this case scattering from one mode into the other is unimportant. Most photons are absorbed in the same polarization state in which they were produced. The emergent intensity can be worked out for each mode separately.

The matrix (36) is nearly diagonal,

$$(\boldsymbol{\alpha} - \boldsymbol{\sigma})\boldsymbol{\alpha} \approx \begin{pmatrix} \kappa_1\alpha_1 & 0 \\ 0 & \kappa_2\alpha_2 \end{pmatrix}, \tag{39}$$

and so is $\boldsymbol{\Lambda}$:

$$\boldsymbol{\Lambda} \approx \begin{pmatrix} (\kappa_1\alpha_1)^{1/2} & 0 \\ 0 & (\kappa_2\alpha_2)^{1/2} \end{pmatrix}, \tag{40}$$

and $\mathbf{C}$:

$$\mathbf{C} \approx \begin{pmatrix} \dfrac{1}{(\kappa_1\alpha_1)^{1/2} + \kappa_1} & 0 \\ 0 & \dfrac{1}{(\kappa_2\alpha_2)^{1/2} + \kappa_2} \end{pmatrix}. \tag{41}$$

If the medium is strongly scattering ($\sigma_i \gg \kappa_1$), one has $\alpha_i \gg \kappa_1$, and thus

$$\mathbf{C} \approx \begin{pmatrix} (\kappa_1\alpha_1)^{-1/2} & 0 \\ 0 & (\kappa_2\alpha_2)^{-1/2} \end{pmatrix}. \tag{42}$$

Because the depths c_{11} and c_{22} are much smaller than $\kappa_1{}^{-1}$ and $\kappa_2{}^{-1}$, the emergent intensities $F_1 \approx 2C_{11}\kappa_1$, $F_2 \approx C_{22}\kappa_2$ are far below the blackbody limits.

b) Intermediate-Coupling Case: $\kappa_1 \ll \sigma_{12} \ll \kappa_2$

Here a photon that was produced in mode 2 is likely to be reabsorbed in state 2. A typical 1-photon, however, will terminate its life by scattering into mode 2. We expect that σ_{12} will play the role of an effective absorption cross section for 1-photons:

$$(\boldsymbol{\alpha} - \boldsymbol{\sigma})\boldsymbol{\alpha} \approx \begin{pmatrix} \sigma_{12}\alpha_1 & -\sigma_{12}\alpha_2 \\ -\sigma_{21}\alpha_1 & \kappa_2\alpha_2 \end{pmatrix}. \tag{43}$$

In terms of its (approximate) eigenvalues, $\lambda \approx (\kappa_2\alpha_2)^{1/2}$ and $\mu \approx (\sigma_{12}\alpha_1)^{1/2}$, the matrix $\boldsymbol{\Lambda}$ can be written in the form

$$\boldsymbol{\Lambda} \approx \begin{pmatrix} \mu & \dfrac{-\mu^2}{\lambda}\dfrac{\alpha_2}{\alpha_1} \\ \dfrac{-\mu^2}{\lambda} & \lambda \end{pmatrix} \approx \begin{pmatrix} (\sigma_{12}\alpha_1)^{1/2} & -\sigma_{12}(\alpha_2/\kappa_2)^{1/2} \\ 0 & (\kappa_2\alpha_2)^{1/2} \end{pmatrix}. \tag{44}$$

For the matrix $\mathbf{C}$ we obtain finally

$$\mathbf{C} \approx \begin{pmatrix} \dfrac{1}{\kappa_1 + (\sigma_2\alpha_1)^{1/2}} & \dfrac{1}{\kappa_2[1 + (\alpha_1/\sigma_{12})^{1/2}]} \\ \dfrac{1}{[\kappa_2 + (\kappa_2\alpha_2)^{1/2}][1 + (\alpha_1/\sigma_{12})^{1/2}]} & \dfrac{1}{\kappa_2 + (\kappa_2\alpha_2)^{1/2}} \end{pmatrix}. \tag{45}$$

c) Strong-Coupling Case: $\sigma_{12} \gg \kappa_1, \kappa_2$

If this condition is satisfied, every photon is scattered many times from one mode into the other. When it escapes, it retains no memory of which mode it was produced in. Hence we expect $C_{11} \approx C_{12}$ and $C_{21} \approx C_{22}$.

The matrix $\boldsymbol{\alpha} - \boldsymbol{\sigma}$ is nearly singular; correspondingly one has to retain a few more terms than in the preceding cases in order not to run into trouble when taking the inversion matrix in equation (35). The determinant of $\boldsymbol{\Lambda}^2$ is

$$\det(\boldsymbol{\Lambda}^2) = \lambda^2\mu^2 \approx (\kappa_1 + \kappa_2)\sigma_{12}\alpha_1\alpha_2\,, \tag{46}$$

and the eigenvalues λ, μ of $\boldsymbol{\Lambda}$ are

$$\lambda \approx \left[\frac{(\kappa_1 + \kappa_2)\alpha_1\alpha_2}{\alpha_1 + \alpha_2}\right]^{1/2} \quad \text{and} \quad \mu \approx [\sigma_{12}(\alpha_1 + \alpha_2)]^{1/2}\,. \tag{47}$$

Using these expressions, and $\lambda \ll \mu$, we find

$$\mathbf{\Lambda} \approx \begin{pmatrix} \lambda + \dfrac{\sigma_{21}\alpha_1}{\mu} & -\dfrac{\sigma_{12}\alpha_2}{\mu} \\ -\dfrac{\sigma_{21}\alpha_1}{\mu} & \lambda + \dfrac{\sigma_{12}\alpha_2}{\mu} \end{pmatrix} . \tag{48}$$

Keeping only terms of order λ/σ_{12}, i.e., of order $(\kappa/\sigma_{12})^{1/2}$, one arrives at

$$\mathbf{\Lambda} + \boldsymbol{\alpha} - \boldsymbol{\sigma} \approx \begin{pmatrix} \sigma_{21} + \lambda + \dfrac{\sigma_{21}\alpha_1}{\mu} & -\sigma_{12} - \dfrac{\sigma_{12}\alpha_2}{\mu} \\ -\sigma_{21} - \dfrac{\sigma_{21}\alpha_1}{\mu} & \sigma_{12} + \lambda + \dfrac{\sigma_{12}\alpha_2}{\mu} \end{pmatrix} , \tag{49}$$

the determinant of which is

$$\det(\mathbf{\Lambda} + \boldsymbol{\alpha} - \boldsymbol{\sigma}) \approx \lambda(2\sigma_{12} + \mu) . \tag{50}$$

Taking the inverse, and again dropping terms of order λ/σ_{12}, we finally obtain

$$\mathbf{C} \approx \lambda^{-1} \begin{pmatrix} \dfrac{\mu + \alpha_2}{2\mu + \alpha_1 + \alpha_2} & \dfrac{\mu + \alpha_2}{2\mu + \alpha_1 + \alpha_2} \\ \dfrac{\mu + \alpha_1}{2\mu + \alpha_1 + \alpha_2} & \dfrac{\mu + \alpha_1}{2\mu + \alpha_1 + \alpha_2} \end{pmatrix} . \tag{51}$$

As expected, the two columns are equal (within the approximations made). The *total* flux of photons is given simply by

$$F = F_1 + F_2 \approx 2\lambda^{-1}(\kappa_1 + \kappa_2) = \left[\frac{\alpha_1\alpha_2}{(\kappa_1 + \kappa_2)(\alpha_1 + \alpha_2)}\right]^{1/2} . \tag{52}$$

If one mode has a significantly shorter mean free path, say $\alpha_2 \gg \alpha_1$, we can approximate

$$\lambda = x_{\rm th}^{-1} \approx (\kappa_2\alpha_1)^{1/2} , \qquad \mu \approx (\sigma_{12}\alpha_2)^{1/2} , \tag{53}$$

i.e., the thermalization length is controlled by the larger absorption coefficient and the smaller of the two total opacities.

The emergent intensities become

$$\frac{I_2}{B} \sim \lambda^{-1} \frac{\mu + \alpha_1}{2\mu + \alpha_1 + \alpha_2}(\kappa_1 + \kappa_2) \sim \frac{1}{(\kappa_2\alpha_1)^{1/2}} \frac{(\sigma_{12}\alpha_2)^{1/2}}{\alpha_2} \kappa_2 = \left(\frac{\kappa_2}{\alpha_2}\right)^{1/2}\left(\frac{\sigma_{12}}{\alpha_1}\right)^{1/2} ,$$

$$\frac{I_1}{B} \sim \lambda^{-1} \frac{\mu + \alpha_2}{2\mu + \alpha_1 + \alpha_2}(\kappa_1 + \kappa_2) \sim \frac{\kappa_2}{(\kappa_2\alpha_1)^{1/2}} \sim \left(\frac{\kappa_2}{\alpha_1}\right)^{1/2} . \tag{54}$$

The intensity in either mode cannot be larger than the blackbody limit. Also, I_2 must be smaller than B, since we assumed strong coupling, $\sigma_{12} \gg \kappa_{1,2}$, and thus $\kappa_2 \ll \sigma_{12} \lesssim \alpha_1$. The ratio of polarizations turns out to be

$$\frac{I_2}{I_1} \sim \left(\frac{\sigma_{12}}{\alpha_2}\right)^{1/2} .$$

VI. RESULTS AND DISCUSSION

Figures 4–8 depict the numerical evaluation of the exact solution of the transfer problem specified by equations (19) and (20). In Figure 4 we see the typical features of the semi-infinite atmosphere which were discussed qualitatively in § III. The mode of shorter mean free path has the lower intensity in the scattering-dominated regime $\omega > \omega_b$, and follows closely the spectral behavior of the nonmagnetic case. The mode of longer mean free path follows the blackbody behavior, i.e. $I = B$ in the frequency range $\omega_b < \omega < \omega_b'$. Beyond ω_b' the spectrum is flat at low frequencies, and falls off exponentially at high frequencies $\omega > 3kT$. At infinite optical depth a cyclotron line excess above the nonmagnetic behavior is seen at $\omega \approx \omega_H$. The behavior of the spectrum near the line is

$$I \approx \epsilon^{1/2}B(\alpha_1/\alpha_2)^{1/2} \approx \epsilon^{1/2}B\frac{\omega}{|\omega - \omega_H|} ,$$

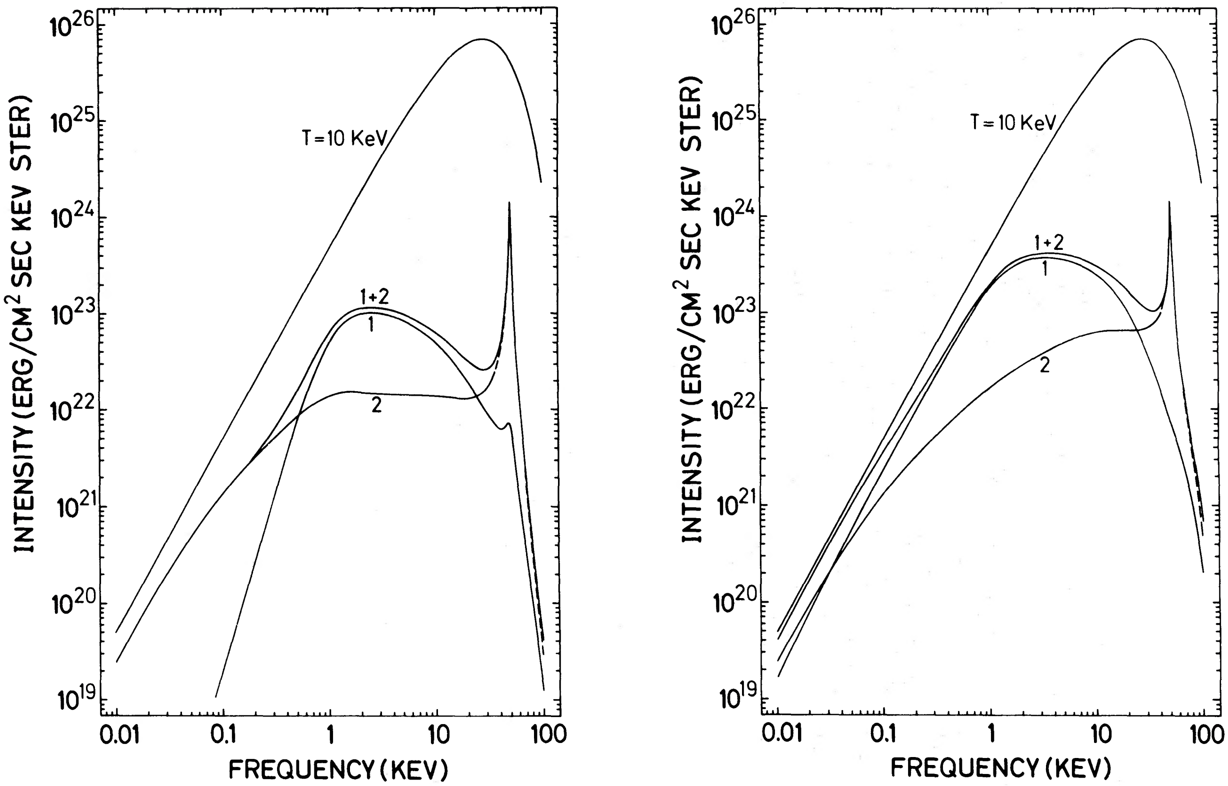

FIG. 5*a* FIG. 5*b*

FIG. 5.—Radiation from a slab of thickness $z_0 = 10^5$ cm, temperature $kT = 10$ keV, and density $n_e = 10^{22}$ cm^{-3}. A strong emission line appears at the cyclotron frequency $\hbar\omega_H = 50$ keV. (*a*) Radiation from the slab itself. (*b*) Spectrum of the same slab if it is illuminated from below with blackbody radiation for temperature 5 keV (not indicated).

if we neglect thermal broadening. Thermal effects will Doppler-broaden this behavior and can be easily accounted for (see Ventura 1979).

Figure 5(*a*) shows the effect of finite optical depth on the spectrum. Taking the same temperature $T = 10$ keV and density $n_e = 10^{22}$ cm^{-3} as before, but a thickness $z_0 = 10^5$ cm, we see a sharp drop in I_1 at low frequencies and a break in I_2 at around 1 keV. The slab is transparent to mode-1 photons for $\omega \ll 1$ keV, at which z_0 is much smaller than the mode's mean free path $\alpha_1{}^{-1}$ (see Fig. 1). At this same frequency range, the slab is optically thick to mode-2 photons, since $x_{\text{th}} \approx \kappa_2{}^{-1} < z_0$, and it follows the $\epsilon^{1/2}B$ behavior. Beyond 1 keV, however, $x_{\text{th}} > z_0$, the slab becomes translucent, and the radiated intensity drops well below the optically thick case. If we now supply a background illumination of a $T_B = 5$ keV Planck flux (Fig. 5*b*) we see an increase of the total intensity, due to translucence above $\omega = 1$ keV, as well as to mode-1 transparency at low frequencies.

Figure 6 shows the transmitted intensity for the illuminated slab of the example above, and also shows the reduced transmission when the slab dimension is increased to $z_0 = 10^6$ cm. The sharp drop in the transmitted intensity at $\omega > 1$ keV is the result of having passed from the translucent to the optically thick regime at these frequencies. In the case $z_0 = 10^6$ cm the spectrum has become a composite of two principal contributions, with the $\omega < 0.35$ keV transparency range and the $\omega > 0.35$ keV self-absorbed range quite distinct from each other. Finally, Figure 7 gives a completely translucent case with parameters $n_e = 10^{20}$ cm^{-3}, $T = 10$ keV, and $z_0 = 10^5$ cm. Every photon produced in the slab is likely to escape since $z_0 < x_{\text{th}}$ in the scattering-dominated regime. Figure 7 gives the intensity of a self-radiating slab (without background illumination), which is equal to the product $(\kappa_1 + \kappa_2)Bz_0$. The effect of a background temperature (10 keV) higher than the slab temperature (5 keV) is shown in Figure 8. Like the Fraunhofer lines in the spectra of normal stars, the cyclotron line appears here in absorption.

a) *Effect of Vacuum Polarization*

In the strong magnetic fields ($B \approx 10^{12}$ gauss) encountered in pulsars (Trümper *et al.* 1978), the vacuum polarization effect of the virtual electron-positron pairs induced by the field can play a dominant role (Mészáros and Ventura 1978, 1979). The radiative cross sections (Thomson, bremsstrahlung, etc.) change their frequency and direction dependence, owing to the fact that the normal mode structure is dominated by the vacuum (see Fig. 1*b*). The most striking manifestation of this is the appearance of a new feature in the cross sections, besides the usual

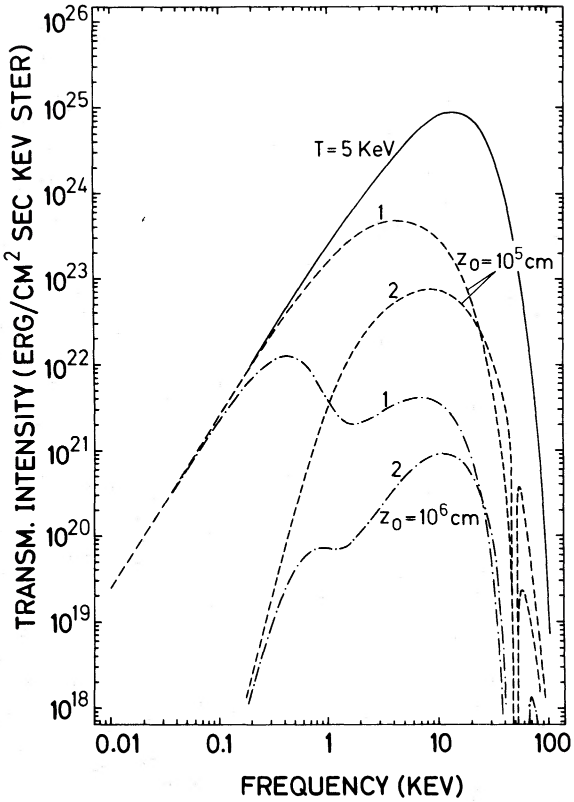

FIG. 6.—Transmitted intensities from a 5 keV background flux incident on a slab of dimension 10^5 cm (*dashed lines*) or 10^6 cm (*solid lines*) and $n_e = 10^{22}$ cm^{-3}. Both cases show a strong cyclotron absorption effect. The self-radiation of the slab is not included here.

cyclotron resonance (Ventura *et al.* 1979), which may lead to another line in the spectrum of an X-ray pulsar. In the present paper we have not included vacuum polarization, since we were more interested in the general behavior of the transfer for arbitrary cross sections. We therefore used the cold-plasma cross sections, which exhibit a simpler behavior (Fig. 1*a*) for the purposes of illustration. There is, however, no difficulty in introducing the vacuum effect in the cross sections, and this in fact is what was done in Paper I.

b) *Effect of Incoherence*

Up to now we have assumed that photons scatter in the slab and escape at precisely the same frequency at which they were created. This assumption is justified only if the number of scatterings suffered prior to escape is much less than the critical number $N_c \equiv mc^2/3kT$. If this number is exceeded, the photon (frequency) distribution is very efficiently altered, leading exponentially to a thermal (Bose-Einstein) distribution within a few times N_c (Kompaneets 1957; Weymann 1965; Cooper 1971). For an electron temperature $T = 10$ keV, $N_c \sim 20$, and this poses a severe limitation on most of the examples treated in the last section. In principle this process of Comptonization is inextricably coupled to the spatial diffusion of photons, and can be treated only through the help of complicated numerical schemes. Very often, however, one deals with limiting cases where the number of scatterings $N \ll N_c$ or $N \gg N_c$. In the first case Comptonization may be viewed as a perturbation on the spatial diffusion problem, while in the second case it is the dominant effect and may again be treated separately. The qualitative aspects for the Comptonization of a continuum by a hot nonmagnetized gas have been summarized convincingly by Felten and Rees (1972), where references to previous literature can be found. The emergent spectra can be very roughly understood as consisting of two independent additive components: (*a*) a coherent spectrum arising within the outermost layer of optical depth $\tau_{es} \sim (mc^2/3kT)^{1/2}$ and (*b*) a thermalized equilibrium distribution of photons originating from deeper layers.

To generalize this argument to the transfer of two polarizations one has to look more closely into the photon histories. It is clear that Comptonization operates in this case mainly through the mode of shorter mean free path. Thus, assuming $\sigma_2 \gg \sigma_1$, the average photon is produced in mode 2 (in the self-radiating case), and is effectively Comptonized before it has a chance to convert to mode 1. This happens because the average number of scatterings prior to mode conversion is $\sigma_2/\sigma_{12} \gg mc^2/3kT$, under the above assumption. Comptonization therefore tends to

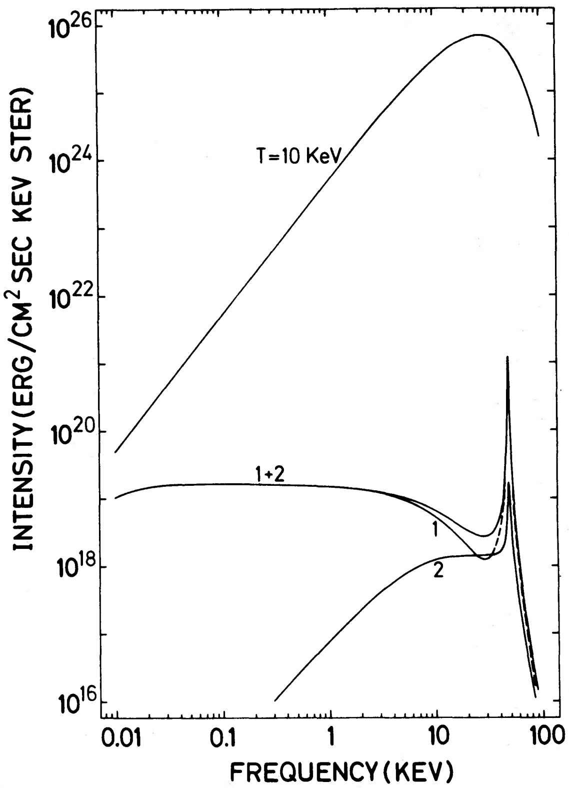

FIG. 7.—Same as Fig. 5, but for a reduced plasma density $n_e = 10^{20}$ cm^{-3}. We see the characteristic optically thin bremsstrahlung spectrum.

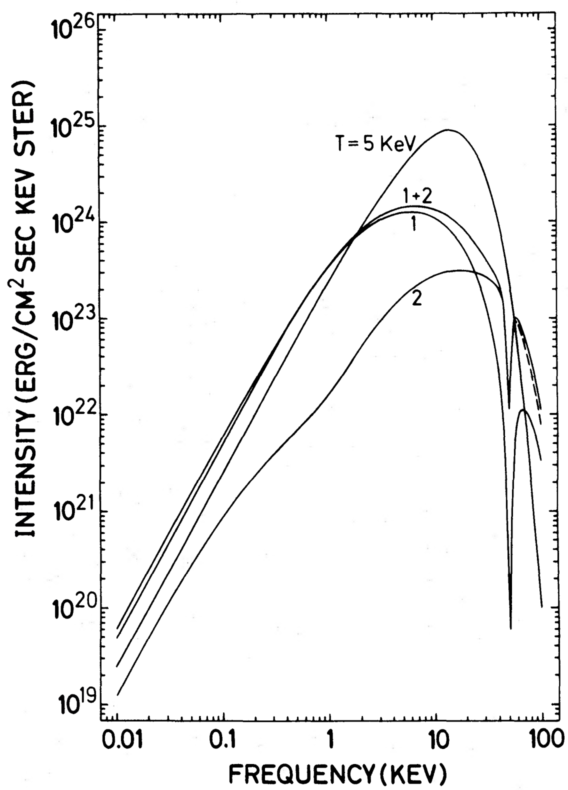

FIG. 8.—Same as Fig. 5(*b*), but with the temperature of the slab (5 keV) lower than that of the illuminating background (10 keV). The cyclotron line now appears as a Fraunhofer-type absorption line.

reduce the importance of mode conversion. This argument can be followed through to give the ground rules for estimating the modification expected on the coherent spectra due to Comptonization. Given the complexity, however, of the transfer problem for polarized radiation, we have chosen to limit our present discussion mainly to an in-depth account of the coherent problem and devote a separate paper to the effects of incoherence.

In the numerical examples discussed, incoherence should also play a principal role in determining the size and shape of the spectral feature near the cyclotron resonance. Analytic studies of some facets of this important problem have been presented recently by Bell, Frisch, and Frisch (1979) and by Bonazzola, Heyvaerts, and Puget (1979). These authors, however, do not take birefringence or spatial diffusion into account, and therefore our approach is complementary to theirs. A generalized treatment of incoherence in a birefringent medium accounting for the line as well as the continuum is still missing.

In conclusion, the transfer of radiation in a strongly magnetized medium, with polarization-dependent opacities, presents some interesting departures from the case of nonpolarizing media. The interplay between the absorption and the polarization-exchange scattering assumes a dominant role, leading to peculiar features, the origin of which remains hidden in typical Monte Carlo simulations. Our aim here has been to gain insight into the details of the transfer, using a simplified atmosphere model, which has the advantage that it allows exact solutions of the radiative transfer equations that lend themselves to comparison with probabilistic and semi-intuitive considerations. One can hope that such analytical studies, coupled to detailed numerical schemes, such as presented recently by Yahel (1979, 1980), will shed light on the physics of the magnetic X-ray sources.

We are indebted to Prof. J. Trümper for useful discussions.

APPENDIX

EXACT SOLUTION OF THE TRANSFER EQUATIONS

Here we give the explicit solutions to the coupled radiative-transfer equations (15), subject to the boundary conditions (20). The eigenvectors u and v can be expressed with the help of their associated eigenvalues λ and μ as follows:

$$\boldsymbol{u} = \begin{pmatrix} \alpha_1 \sigma_{12} \\ \alpha_1(\alpha_1 - \sigma_{11}) - \lambda^2 \end{pmatrix}, \qquad \boldsymbol{v} = \begin{pmatrix} \alpha_1 \sigma_{12} \\ \alpha_1(\alpha_1 - \sigma_{11}) - \mu^2 \end{pmatrix}. \tag{A1}$$

The normalization of these vectors is arbitrary. It is convenient to redefine the coefficients in the general solution, equation (19), and to write it in the form

$$\begin{aligned} \boldsymbol{J} = \boldsymbol{J}^* &- [r_+\{\exp[-\lambda(z_0 - z)] + \exp(-\lambda z)\} + r_-\{\exp[-\lambda(z_0 - z)] - \exp(-\lambda z)\}]\boldsymbol{u} \\ &- [s_+\{\exp[-\mu(z_0 - z)] + \exp(-\mu z)\} + s_-\{\exp[-\mu(z_0 - z)] - \exp(-\mu z)\}]\boldsymbol{v}\,. \end{aligned} \tag{A2}$$

The boundary conditions (20) can be cast into the following form:

$$\frac{1}{2}\left|\boldsymbol{J} - \boldsymbol{\alpha}^{-1}\frac{d}{dz}\boldsymbol{J}\right|_{z=0} = 0\,, \qquad \frac{1}{2}\left|\boldsymbol{J} + \boldsymbol{\alpha}^{-1}\frac{d}{dz}\boldsymbol{J}\right|_{z=z_0} = I_{\rm inc}\,. \tag{A3}$$

Inserting the general solution (A2), this leads to a four-by-four system of linear equations:

$$\begin{pmatrix} A_1 & -A_1' & B_1 & -B_1' \\ A_2 & -A_2' & B_2 & -B_2' \\ A_1 & A_1' & B_1 & B_1' \\ A_2 & A_2' & B_2 & B_2' \end{pmatrix} \begin{pmatrix} r_+ \\ r_- \\ s_+ \\ s_- \end{pmatrix} = \begin{pmatrix} J_1^* \\ J_2^* \\ J_1^* - 2I_{\rm inc_1} \\ J_2^* - 2I_{\rm inc_2} \end{pmatrix}, \tag{A4}$$

where the matrix elements are abbreviations of

$$\begin{aligned} A_i &= \{[1 + \exp(-\lambda z_0)] + [1 - \exp(-\lambda z_0)]\lambda/\alpha_i\}u_i\,, \\ A_i' &= \{[1 - \exp(-\lambda z_0)] + [1 + \exp(-\lambda z_0)]\lambda/\alpha_i\}u_i\,, \\ B_i &= \{[1 + \exp(-\mu z_0)] + [1 - \exp(-\mu z_0)]\mu/\alpha_i\}v_i\,, \\ B_i' &= \{[1 - \exp(-\mu z_0)] + [1 + \exp(-\mu z_0)]\mu/\alpha_i\}v_i\,. \end{aligned} \tag{A5}$$

Adding and subtracting the equations for corresponding polarizations in (A4), and a little reordering, yield

$$\begin{pmatrix} A_1 & B_1 & 0 & 0 \\ A_2 & B_2 & 0 & 0 \\ 0 & 0 & A_1' & B_1' \\ 0 & 0 & A_2' & B_2' \end{pmatrix} \begin{pmatrix} r_+ \\ s_+ \\ r_- \\ s_- \end{pmatrix} = \begin{pmatrix} J_1^* - I_{\text{inc}_1} \\ J_2^* - I_{\text{inc}_2} \\ -I_{\text{inc}_1} \\ -I_{\text{inc}_2} \end{pmatrix} . \tag{A6}$$

Defining $D = A_1B_2 - A_2B_1$ and $D' = A_1'B_2' - A_2'B_1'$, the coefficients $r_\pm, s_\pm$ are easily expressed in the form

$$\begin{aligned} Dr_+ &= B_2(J_1^* - I_{\text{inc}_1}) - B_1(J_2^* - I_{\text{inc}_2}) , \\ Ds_+ &= A_1(J_2^* - I_{\text{inc}_2}) - A_2(J_1^* - I_{\text{inc}_1}) , \\ D'r_- &= B_1'I_{\text{inc}_2} - B_2'I_{\text{inc}_1} , \\ D's_- &= A_2'I_{\text{inc}_1} - A_1'I_{\text{inc}_2} . \end{aligned} \tag{A7}$$

From the boundary condition for $z = 0$ (no radiation from above) it follows that the emergent intensities can be found from

$$\boldsymbol{I}^+(0) = \boldsymbol{J}(0) = \boldsymbol{\alpha}^{-1}\left|\frac{d}{dz}\boldsymbol{J}\right|_{z=0} . \tag{A8}$$

Using the second form we get

$$\begin{aligned} \boldsymbol{I}^+(0) = \{r_+[1 - \exp(-\lambda z_0)] - r_-[1 + \exp(-\lambda z_0)]\}\lambda\boldsymbol{\alpha}^{-1}\boldsymbol{u} \\ + \{s_+[1 - \exp(-\mu z_0)] - s_-[1 + \exp(-\mu z_0)]\}\mu\boldsymbol{\alpha}^{-1}\boldsymbol{v} . \end{aligned} \tag{A9}$$

The radiation originating in the slab itself is found by letting $\boldsymbol{I}_{\text{inc}} = 0$. The self-radiation part of equation (A7) is

$$r_+^* = (B_2J_1^* - B_1J_2^*)/D , \qquad s_+^* = (A_1J_2^* - A_2J_1^*)/D , \tag{A10}$$

and equation (A9) reduces to

$$\boldsymbol{I}^+(0) = r_+^*[1 - \exp(-\lambda z_0)]\lambda\boldsymbol{\alpha}^{-1}\boldsymbol{u} + s_+^*[1 - \exp(-\mu z_0)]\mu\boldsymbol{\alpha}^{-1}\boldsymbol{v} . \tag{A11}$$

REFERENCES

Bell, T., Frisch, H., and Frisch, U. 1979, *Phys. Rev.*, in press.
Bonazzola, S., Heyvaerts, J., and Puget, J. L. 1979, *Astr. Ap.*, **78**, 53.
Canuto, V., Lodenquai, J., and Ruderman, M. 1971, *Phys. Rev. D.*, **3**, 2303.
Chandrasekhar, S. 1960, *Radiative Transfer* (New York: Dover).
Cooper, G. 1971, *Phys. Rev. D*, **3**, 2312.
Felten, J. E., and Rees, M. J. 1972, *Astr. Ap.*, **17**, 226.
Ginzburg, V. L., Sazonov, V. N., and Syrovatsky, S. I. 1968, *Soviet Phys. Upsekhi*, **11**, 34.
Gnedin, Yu. N., and Pavlov, G. G. 1974, *Soviet Phys.—JETP*, **38**, 903.
Gnedin, Yu. N., Pavlov, G. G., and Shibanov, Yu. A. 1978, *Soviet Astr. Letters*, **4**, 117.
Gnedin, Yu. N., and Sunyaev, R. A. 1973, *Soviet Phys.—JETP*, **38**, 51.
Jones, C. 1977, *Ap. J.*, **214**, 856.
Kompaneets, A. S. 1957, *Soviet Phys.—JETP*, **4**, 730.
Lamb, F. K., and Sutherland, P. G. 1974, in *IAU Symposium No. 53, Physics of Dense Matter*, ed. C. J. Hansen (Dordrecht: Reidel), p. 265.
Lodenquai, J., Canuto, V., Rudermann, M., and Tsuruta, S. 1974, *Ap. J.*, **190**, 141.
Markert, T. H., *et al.* 1979, *Ap. J. Suppl.*, **39**, 573.
Masters, A. R., Fabian, A. C., Pringle, J. E., and Rees, M. J. 1977, *M.N.R.A.S.*, **178**, 501.
Mészáros, P., and Ventura, J. 1978, *Phys. Rev. Letters*, **41**, 1544.
———. 1979, *Phys. Rev. D*, **19**, 3565.
Nagel, W. 1980, *Ap. J.*, in press.
Ostriker, J. P. 1977, *Ann. NY Acad. Sci.*, **302**, 229.
Pacholczyk, A. G. 1977, *Radio Galaxies* (Oxford: Pergamon).
Schreier, E., Giacconi, R., Gursky, H., Kellog, E., and Tananbaum, H. 1972, *Ap. J.* (*Letters*), **178**, L71.
Sobolev, V. V. 1963, *A Treatise on Radiative Transfer* (Princeton: van Nostrand).
Trümper, J., Pietsch, W., Reppin, C., Voges, W., Staubert, R., and Kendziorra, E. 1978, *Ap. J.* (*Letters*), **219**, L105.
Ventura, J. 1979, *Phys. Rev. D*, **19**, 1684.
Ventura, J., Nagel, W., and Mészáros, P. 1979, *Ap. J.* (*Letters*), **233**, L125 (Paper I).
Voges, W., Pietsch, W., Reppin, C., Trümper, J., Kendziorra, E., and Staubert, R. 1979, (*Cospar*) *X-ray Astronomy*, ed. W. A. Baity and L. E. Peterson (Oxford: Pergamon), p. 485.
Weymann, R. 1965, *Phys. Fluids*, **8**, 2112.
Wheaton, Wm. A., *et al.* 1979, *Nature*, **282**, 240.
Yahel, R. 1979, *Ap. J.* (*Letters*), **229**, L73.
———. 1980, *Ap. J.*, in press.
Zheleznyakov, V. V. 1970, *Radio Emission of the Sun and Planets* (New York: Pergamon).

P. Mészáros: NASA Goddard Space Flight Center, Laboratory for High Energy Astrophysics, Code 660, Greenbelt, MD 20771

W. Nagel and J. Ventura: Max-Planck-Institut für Physik und Astrophysik, Institut für Extraterrestrische Physik, 8046 Garching bei München, Federal Republic of Germany